Neutral-Axis Position Based Damage Detection of Bridge Deck Using Strain Measurement: Numerical and Experimental Verifications

Y. Q. NI, H. W. XIA, X. W. YE

ABSTRACT

This paper provides numerical and experimental studies on using the neutral-axis position as a damage index for bridge deck condition assessment. A beam-like deck model subjected to moving bogies is fabricated with crack damage of different extents incurred on a designated cross-section. Making use of a Kalman filter (KF) estimator which is specifically formulated to estimate the neutral-axis position from traffic-induced strain responses, numerical simulations and experiments of the deck model are conducted to verify the sensitivity of the neutral-axis position based damage detection technique to crack damage and the capability of this technique for locating damage. The robustness of the KF estimator is examined under different boundary conditions and under static and moving loads. Both the numerical and experimental results show that the neutral-axis position is highly sensitive to local damage on deck sections and can as well serve as an indicator of damage location when strain sensors are densely instrumented.

INTRODUCTION

In-service bridge structures are at risk from structural degradation, service demands of increasing traffic flow and heavier truck loads, natural or man-made disasters, or deferred maintenance. Condition assessment of these public facilities for future serviceability and safety is a challenging task to their owners and engineers. Long-term structural health monitoring (SHM), on a continuous basis, can offer a chance to track structure status evolutionarily and thus early warnings could be signaled before catastrophic failure happens [1, 2]. Integrating SHM data into procedures of structural

Y. Q. Ni*, H. W. Xia, X. W. Ye, Department of Civil and Structural Engineering, The Hong Kong Polytechnic University, Hong Kong (ceyqni@polyu.edu.hk).

condition assessment is envisioned to achieve objective and quantitative condition assessment for in-service bridges. Structural condition assessment using continuously monitored strains has been receiving more and more attentions [3-5], especially when distributed strain monitoring systems are available [6-8].

The neutral-axis position has been considered as a damage indicator for bridge deck assessment on the premise that it shifts when damage occurs [3, 9]. Under traffic loads, bending behavior dominates the response of beam-like bridge deck. When the traffic-induced strain responses at the top and bottom of a deck section are measured, the neutral-axis position can be estimated. A Kalman filter (KF) estimator for locating the neutral-axis position from measured strains has been developed and its robustness under different levels of measurement noise and varying traffic load patterns has been validated in the companion paper [10]. The present study aims to verify its capability to detect and locate crack damage on bridge deck through numerical and experimental studies. A model of bridge deck is fabricated for this purpose. Numerical simulations and experiments are conducted on the deck model to identify the shift in the neutral-axis position estimated by the strain responses obtained at different deck sections under various damage severities. The robustness of the KF estimator is also examined under different boundary conditions and under static and moving loads.

ESTIMATION OF NEUTRAL-AXIS POSITION

Beam-like bridge deck behaves like a flexural beam when traffic loads cause it to bend. When the strain responses at the top and bottom points of a deck section are measured, the neutral-axis position in ratio can be estimated by

$$r = \frac{\varepsilon_b}{\varepsilon_b + \varepsilon_t} \tag{1}$$

where ε_b and ε_t are the strains at the bottom and top locations of the deck section, respectively. By taking the neutral-axis position in ratio as a state variable, the discrete KF equation can be obtained as [9]

$$\hat{r}_k = \Phi_k \hat{r}_{k-1} + K_k (z_k - H\Phi_k \hat{r}_{k-1}) \tag{2}$$

where $\hat{r}_k$ is an estimate of the state r_k at time k (the kth sampling instant); Φ_k is the propagation scalar that propagates the state from one sampling instant to the next; K_k is the KF gain that minimizes the variance of the error in the estimate; and H is the measurement scalar that relates the state to the observation z_k.

The KF gain is chosen to minimize the variance of the error in the estimate. The optimal gain at each sampling instant is achieved by an iterative algorithm [9]. With the measured strain response sequences at the top and bottom locations of a deck section, the observation of the state r at each sampling instant is obtained by Equation (1) and then its KF-based estimate is obtained by Equation (2).

SCALE MODEL OF BRIDGE DECK

Figure 1 illustrates the scale model of bridge deck. It is 6 m long with H-shaped section. The material grade is BS4360-43A with an elastic modulus of 205 GPa and a Poisson's ratio of 0.3. In the experiments, strain gauges are deployed at the top and bottom of sections A to C to measure the strain responses under static and moving loads. In the numerical simulations, it is assumed that the strain responses at the top and bottom of the three sections are available. Both simply-supported and fixed-ended boundary conditions are considered for comparison.

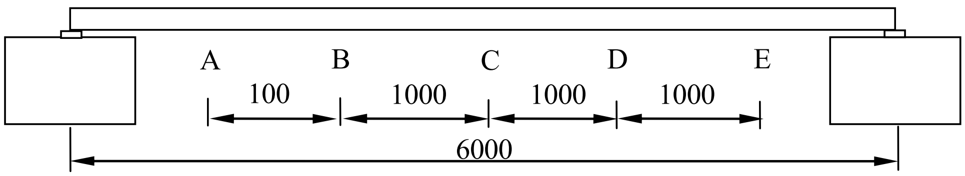

(Unit: mm)

Figure 1. Scale model of bridge deck and sections with strains obtained.

NUMERICAL SIMULATIONS

A multi-scale finite element model of the structure has been formulated with the commercial software ANSYS. In this model 3D solid elements are adopted; and to achieve a compromise between computational precision and efficiency, the structural portion in the vicinity of damage is modeled by fine elements with small mesh size while the portions beyond the damage region are modeled by coarse elements with relatively large mesh size. Two extents of damage, respectively with cuts of 5 mm deep and 15 mm deep on section C from the bottom, are considered in both numerical and experimental studies. The damage is simulated in the finite element model by releasing the connection between adjacent elements at the damage location.

Static Load Case

In the static load case, a concentrated force is applied on the finite element model at section D. With the calculated strains at the top and bottom of the three designated sections, the neural-axis position is estimated in three scenarios: (i) undamaged, (ii) 5 mm damage, and (iii) 15 mm damage. Table 1 shows the estimated results, in which the figures in parentheses denote the relative reduction of the neural-axis position on a specific section due to the presence of damage. It is observed that shift in the neutral-axis position for sections A, B and C is 0.38%, 0.96% and 3.19%, respectively, in the 5 mm damage scenario. In the 15 mm damage scenario, it is 1.84%, 2.98% and 12.00%, respectively.

Table 1. Estimated Neutral-Axis Positions in Static Load Simulation.

Damage condition	Neutral-axis position (ratio)		
	Section A	Section B	Section C
Undamaged	0.50006	0.50003	0.50004
5 mm damage	0.49818 (0.38%)	0.49524 (0.96%)	0.48409 (3.19%)
15 mm damage	0.49087 (1.84%)	0.48514 (2.98%)	0.44000 (12.00%)

Moving Load Case

In the moving load case, a concentrated moving force is applied on the finite element model from one end to the other, and the corresponding time-varying strain responses at the top and bottom of the three designated sections are obtained for KF estimation of the neutral-axis position. To testify whether the neutral-axis position is sensitive to load patterns, different load weights and moving speeds are considered in the undamaged scenario. The simulation results indicate that the estimated neutral-axis position keeps almost unchanged with varying load weight and under different moving speeds.

After verifying the independence of neutral-axis position on load patterns, damage detection study using the finite element model is conducted. For the three scenarios, KF estimation of the neutral-axis position for the designated sections is obtained as shown in Table 2. It is found that shift in the neutral-axis position for sections A, B and C is 0.48%, 0.80% and 3.36%, respectively, in the 5 mm damage scenario. In the 15 mm damage scenario, it is 2.06%, 3.22% and 13.83%, respectively.

Table 2. Estimated Neutral-Axis Positions in Moving Load Simulation.

Damage condition	Neutral-axis position (ratio)		
	Section A	Section B	Section C
Undamaged	0.5006	0.5003	0.5004
5 mm damage	0.4982 (0.48%)	0.4963 (0.80%)	0.4836 (3.36%)
15 mm damage	0.4903 (2.06%)	0.4842 (3.22%)	0.4312 (13.83%)

EXPERIMENTAL VERIFICATIONS

ESG sensors (TML PFL-10-11) and data acquisition equipment (NI SCXI-1000) were used for strain measurements during the experiment. The maximum sampling rate of the ESG interrogator is 1000 Hz and the gauge length is 10 mm. A total of 12 ESG sensors were installed on sections A, B, and C. In the experiment, traffic loading is simulated by a test bogie which is self-driven and controlled by an electro-circuit system. Four load weights, namely 89 kg, 131 kg, 157 kg and 257 kg, are considered in the experiment for moving load simulation. Figure 2 illustrates the strain gauges deployed on the test structure and the bogie for vehicle simulation.

Figure 2. Deployment of strain gauges and bogie for vehicle simulation.

Calibration of Neutral-Axis Position

Before the damage detection test, calibration of neutral-axis position with respect to different boundary conditions is conducted. Strain responses at the top and bottom of the instrumented sections A, B and C for the simply-supported test structure and the fixed-ended test structure under the same moving load are acquired. Then, the neural-axis position is estimated from the acquired strain data by directly using Equation (1) (denoted as the direct method) and by the formulated KF estimator (denoted as the KF method), respectively. Figure 3 illustrates the estimated neural-axis position by the direct and KF methods under the two support conditions. It is observed that the neural-axis position estimation results by the KF method are much more consistent and reliable than those obtained by the direct method. The neutral-axis position estimated by the KF method is 0.5034 and 0.5046, respectively, for the two boundary conditions. The difference is only 0.23%, implying that different boundary conditions have little effect on the estimation of neutral-axis position.

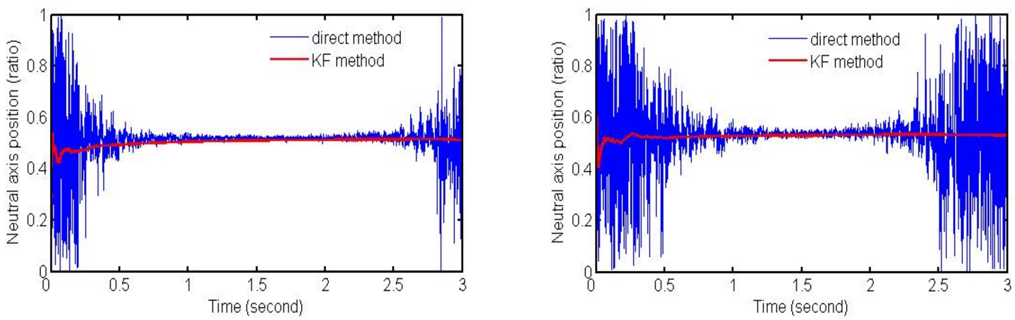

(a) Simply-supported *(b) Fixed-ended*

Figure 3. Estimated neutral-axis positions under different boundary conditions.

Moving Load Tests

Moving load tests are conducted on the test structure before and after incurring damage at the mod-span section. Figure 4 shows the measured strain time histories at the top and bottom of the instrumented sections A, B and C for the fixed-ended test structure under a moving load. Making use of the measured strain responses under different damage conditions, neutral-axis position is estimated by using the direct method and the KF method, respectively. Figure 5 illustrates the estimated results of the neutral-axis position in three scenarios: (i) undamaged, (ii) 5 mm damage, and (iii) 15 mm damage. It is seen that the neutral-axis position estimated by the KF method effectively reflects the damage conditions of the test structure.

Table 3 provides a comparison of the estimated results of neutral-axis position at the three instrumented sections by the KF method (the figures in parentheses denote the relative reduction of the neural-axis position on a specific section due to the presence of damage). In the 5 mm damage scenario, the relative reduction of the neutral-axis position at the three sections is 0.43%, 0.92% and 3.58%, respectively. In the 15 mm damage scenario, it is 2.15%, 2.14% and 10.96%, respectively. These results validate that neutral-axis position is sensitive enough for damage detection. In addition, it is observed that the sensitivity of neutral-axis position to local damage decreases dramatically as it is away from the damaged section. Therefore, the neutral-axis position can also serve as an indicator of damage location. With the development of distributed sensing technology (such as distributed Brillouin optical fiber sensors), the limitation of spatial resolution in strain monitoring can be overcome.

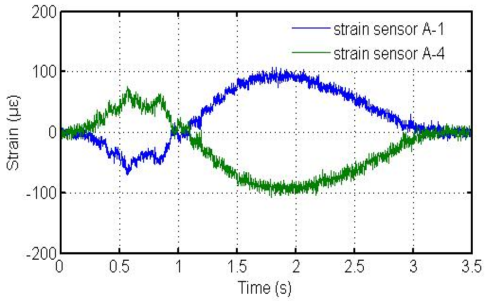

(a) Section A

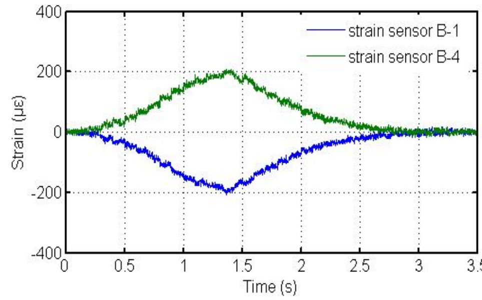

(b) Section B

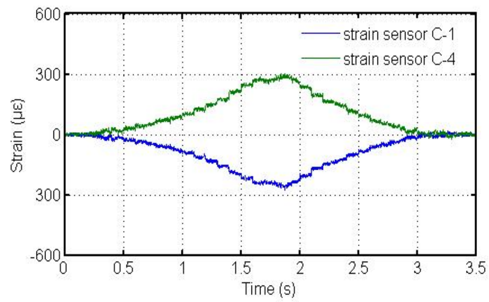

(c) Section C

Figure 4. Measured strain responses under the action of a moving load.

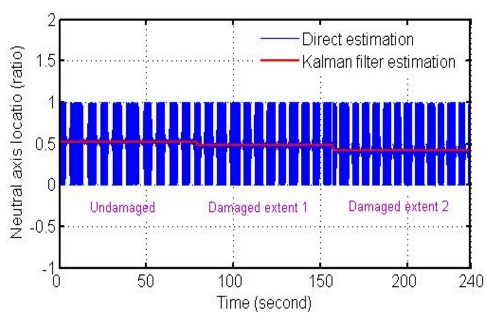

Figure 5. Estimated neutral-axis positions under different damage conditions.

Table 3. Estimated Neutral-Axis Positions in Moving Load Tests.

Damage condition	Neutral-axis position (ratio)		
	Section A	Section B	Section C
Undamaged	0.5061	0.5092	0.5054
5 mm damage	0.5039 (0.43%)	0.5045 (0.92%)	0.4873 (3.58%)
15 mm damage	0.4952 (2.15%)	0.4983 (2.14%)	0.4500 (10.96%)

CONCLUSIONS

Numerical and experimental studies of a neutral-axis position based technique for damage detection of bridge deck have been explored in this paper. A KF estimator has been formulated to estimate the neutral-axis position of bridge deck sections from the measurement data of traffic-induced strains at the top and bottom of the sections. It is found that the estimated neutral-axis position is insensitive to traffic load patterns (different moving load weights and moving speeds). The change of the neutral-axis position estimated on the section close to damage location is significant and large enough to alarm damage; while the neutral-axis position estimated on the sections away from damage location is insensitive to damage. In conclusion, the neutral-axis position estimated by the KF method from strain measurements is a good indictor of local damage incurred in bridge deck and can help locate damage as well.

ACKNOWLEDGMENTS

The work described in this paper was supported by The Hong Kong Polytechnic University under Grant Nos. G-U845 and 1-BB68.

REFERENCES

1. J.M. Ko, and Y.Q. Ni, Design of a structural health monitoring system for long-span bridges, Engineering Structures 3 (2005) 169-185.
2. J.M.W. Brownjohn, Structural health monitoring of civil infrastructure, Philosophical Transactions of the Royal Society A 365 (2007) 589-622.
3. A.J. Cardini, and J.T. DeWolf, Long-term structural health monitoring of a multi-girder steel composite bridge using strain data, Structural Health Monitoring 8 (2009) 47-58.
4. M.L. Wang, and J. Yim, Sensor enriched infrastructure system, Smart Structures and Systems 6 (2010) 309-333.
5. Y.Q. Ni, H.W. Xia, K.Y. Wong, and J.M. Ko, In-service condition assessment of bridge deck using long-term monitoring data of strain response, ASCE Journal of Bridge Engineering 18 (2012) (in press).
6. G. Chen, H. Mu, D. Pommerenke, and J.L. Drewniak, Damage detection of reinforced concrete beams with novel distributed crack/strain sensors, Structural Health Monitoring 3 (2004) 225-243.
7. S. Li, and Z. Wu, Development of distributed long-gage fiber optic sensing system for structural health monitoring, Structural Health Monitoring 6 (2007) 133-143.
8. X. Bao, and L. Chen, Recent progress in Brillouin scattering based fiber sensors, Sensors 11 (2011), 4152-4187.
9. H.W. Xia, SHM-based condition assessment of in-service bridge structures using strain measurement, Ph.D. Thesis, Department of Civil and Structural Engineering, The Hong Kong Polytechnic University, Hong Kong, 2012.
10. H.W. Xia, Y.Q. Ni, and X.W. Ye, Neutral-axis position based damage detection of bridge deck using strain measurement: formulation of a Kalman filter estimator, Proceedings of the 6th European Workshop on Structural Health Monitoring, Dresden, Germany, 2012.